ACS Energy LETTERS

http://pubs.acs.org/journal/aelccp

LETTER

Protection and Reactivation of the [NiFeSe] Hydrogenase from *Desulfovibrio vulgaris* Hildenborough under Oxidative Conditions

Adrian Ruff,*[,†] Julian Szczesny,[†] Sónia Zacarias,[‡] Inês A. C. Pereira,[‡] Nicolas Plumeré,[§] and Wolfgang Schuhmann*[,†]

[†]Analytical Chemistry - Center for Electrochemical Sciences (CES), Ruhr-Universität Bochum, Universitätsstrasse 150, D-44780 Bochum, Germany

[‡]Instituto de Tecnologia Quimica e Biologica Antonio Xavier, Universidade Nova de Lisboa, 278o-157 Oeiras, Portugal

[§]Center for Electrochemical Sciences (CES) - Molecular Nanostructures, Ruhr-Universität Bochum, Universitätsstrasse 150, D-44780 Bochum, Germany

Supporting Information

ABSTRACT: We report on the fabrication of bioanodes for H_2 oxidation based on [NiFeSe] hydrogenase. The enzyme was electrically wired by means of a specifically designed low-potential viologen-modified polymer, which delivers benchmark H_2 oxidizing currents even under deactivating conditions owing to efficient protection against O_2 combined with a viologen-induced reactivation of the O_2 inhibited enzyme. Moreover, the viologen-modified polymer allows for electrochemical co-deposition of polymer and biocatalyst and, by this, for control of the film thickness. Protection and reactivation of the enzyme was demonstrated in thick and thin reaction layers.

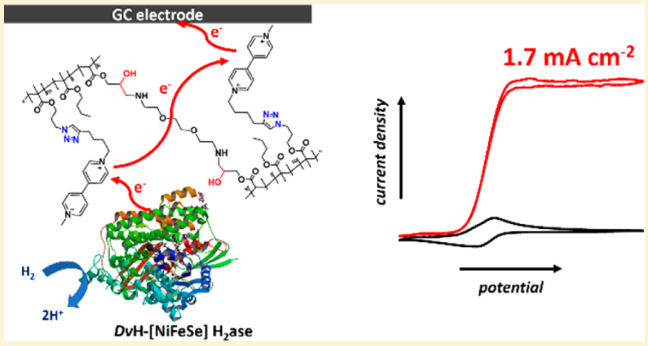

Hydrogenases bearing the [NiFeSe] active site are of particular interest for energy conversion because of their ability to produce H_2 in the presence of certain amounts of O_2.[1−7] This behavior was attributed to their unique structural and chemical properties, which are related to the selenocysteine ligand coordinating the Ni−Fe active site.[7−10] Under rather mild reducing conditions (≈ < 0 V vs SHE) and in a direct electron transfer (DET) regime between an adsorbed enzyme and electrode surface, the inactive enzyme is reduced and full activity is restored.[2,11,12] Consequently, [NiFeSe] hydrogenases show very fast rates of reactivation in the presence of O_2 under reducing conditions (H_2 production). Hence, these types of hydrogenases are very promising catalysts for H_2 evolution, and they have been successfully employed as active material in photocatalytic hydrogen production devices.[3−6,13]

On the other hand, the fast reactivation rate at negative potentials is accompanied by fast deactivation under both oxidizing electrochemical and aerobic conditions.[2,9,11] Hence, the application of [NiFeSe] hydrogenases as biocatalysts in bioanodes was considered unpractical,[2] despite the fact that [NiFeSe] hydrogenases have among the highest activities toward the oxidation of H_2 (up to 4000 s^{-1} for [NiFeSe] from *Desulfomicrobium baculatum*).[2]

We demonstrated recently that fragile catalysts such as highly O_2-sensitive [NiFe] or [FeFe] hydrogenases can be protected from inactivation by O_2 by their incorporation into an oxygen-reducing redox matrix, for example, a viologen-modified redox hydrogel.[14−16] Electrons that are generated by the conversion of H_2 into protons are transferred to the polymer-bound viologen moieties and are used to reduce incoming O_2 at the polymer−electrolyte interface.[14−16] The reduced viologens were also proposed to reactivate O_2 deactivated NiFe hydrogenase when a considerable amount of H_2 was present.[17] Moreover, viologen-based polymers act as a Nernst buffer and protect the hydrogenases from high potential deactivation.[14]

Stimulated by these results, we use the highly active [NiFeSe] hydrogenase from *Desulfovibrio vulgaris* Hildenborough (*Dv*H-[NiFeSe], recombinant form, H_2 uptake activity: 2400 s^{-1})[18] to set a new benchmark for H_2 oxidation currents with a fragile enzyme in a stabilizing redox polymer matrix. We demonstrate that the concept based on thick redox polymer films with O_2 blocking properties[14−16] is transposable to the efficient protection of [NiFeSe] hydrogenase. More

Received: February 26, 2017
Accepted: April 3, 2017
Published: April 3, 2017

DOI: 10.1021/acsenergylett.7b00167
ACS Energy Lett. 2017, 2, 964−968

Scheme 1. Synthesis and Electrochemical Induced Cross-linking Process of the Viologen-Modified Redox Hydrogel P(N_3MA-BA-GMA)-vio[a]

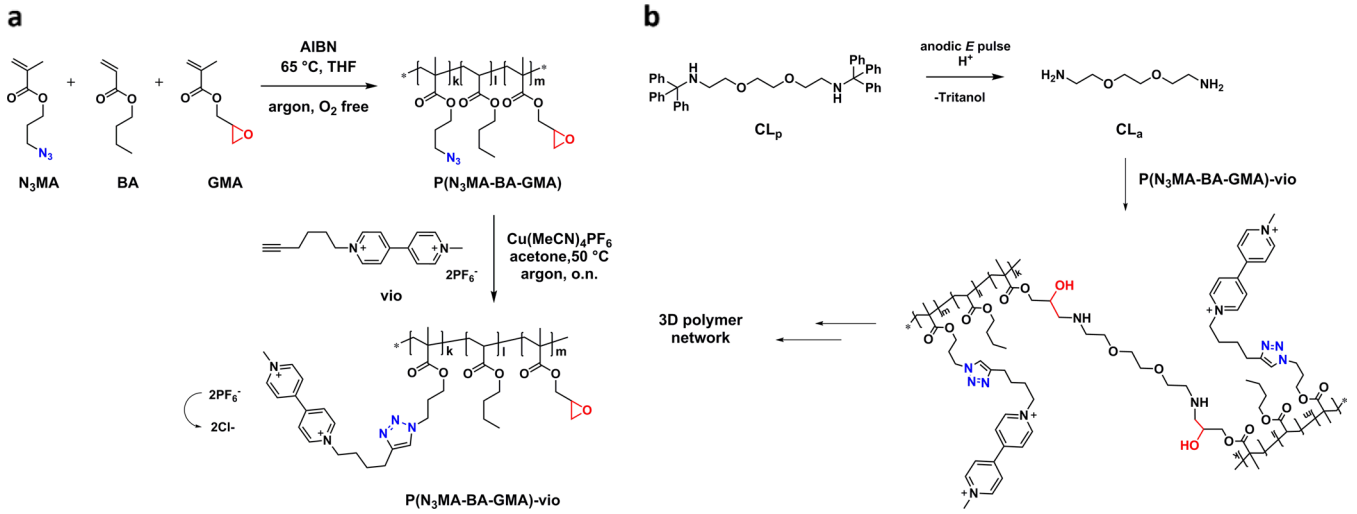

[a](a) The polymer backbone **P(N_3MA-BA-GMA)** was synthesized in a free radical polymerization reaction with the co-monomers **N_3MA** (azidopropyl methacrylate), **BA** (butyl acrylate), and **GMA** (glycidyl methacrylate); M_n(P(N_3MA-BA-GMA)) = 15 kDa, PDI = 2.1 (determined from size exclusion chromatography); composition determined by NMR: k = 71 mol %, l = 20 and 9 mol %. (b) Proposed mechanism for the electrochemical-induced cross-linking process.

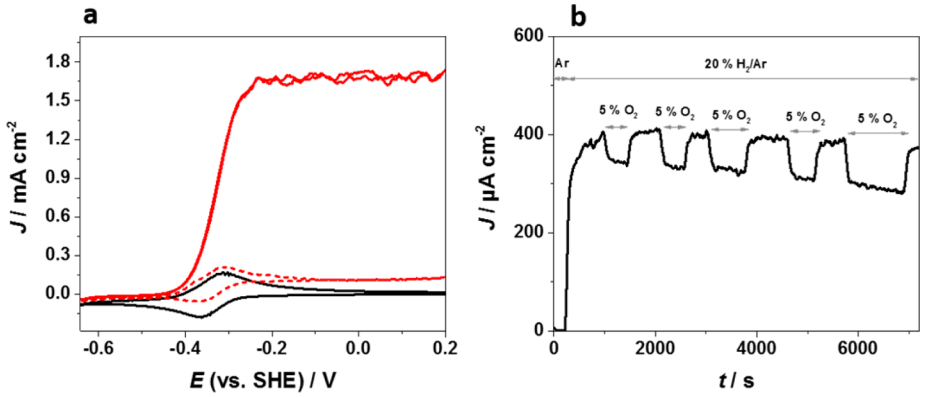

Figure 1. Cyclic voltammograms (a) and chronoamperogram (b) of a thick P(N_3MA-BA-GMA)-vio/*Dv*H-[NiFeSe] film drop cast onto a GC electrode under H_2/O_2/Ar mixtures; working electrolyte: PB (0.1 M, pH 7.4); nominal polymer loading: 69 μg cm^{-2}; nominal enzyme loading: 21 μg cm^{-2}. (a) Scan rate: 10 mV s^{-1}; black line: 100% argon bubbling through the cell; red solid line: 100% H_2; red dashed line: 5% H_2/95% Ar. (b) Applied potential: + 160 mV vs SHE.

importantly, by exploiting specifically designed thin polymer/enzyme films, we reveal the previously unknown reactivation capability through the redox matrix, which is essential for catalysts displaying fast oxidative deactivation rates such as the [NiFeSe] hydrogenase.

We implemented a novel viologen-modified polymer, which allows for the formation of enzyme/polymer films by means of a standard drop cast (*thick films*) and of an electrochemically induced deposition process (*thin films*). The latter is based on the in situ deprotection of protected bifunctional cross-linkers.[19] For this, the polymer backbone **P(N_3MA-BA-GMA)** was synthesized in a multistep synthesis strategy starting from the monomers **N_3MA**, **GMA**, and **BA** in a nominal ratio of 80:10:10, respectively (Scheme 1; for synthesis of the **N_3MA** monomer, see the SI). Analysis of the integrals in the ^{1}H NMR spectrum of the polymer backbone (Figure S1a) revealed an actual composition of 71:20:9, which slightly deviates from the nominal composition derived from the monomer ratio. The polymer backbone bears two functionalities, that is, N_3 (Scheme 1a, blue) and epoxide (red) groups, which allow for covalent attachment of an alkyne-modified viologen derivative and reaction with bifunctional cross-linkers, respectively.

The alkyne-modified viologen-based redox mediator **vio** (Scheme 1; for synthesis, see the SI) was attached to the polymer backbone **P(N_3MA-BA-GMA)** in a Cu(I)-catalyzed 1,3-dipolar cycloaddition ("click" chemistry) to yield the target redox polymer **P(N_3MA-BA-GMA)-vio**. NMR and IR characterization of **P(N_3MA-BA-GMA)-vio** (Figure S1b,c) confirm successful formation of the redox polymer.

Cyclic voltammograms of a drop-cast **P(N_3MA-BA-GMA)-vio** film in 0.1 M phosphate buffer (PB) at pH 7.4 show two chemically reversible redox couples with midpoint potentials of −295 and −660 mV vs SHE, respectively (Figure S2). The potential of the first reduction is above the $H_2/2H^+$ couple (≈−450 mV at pH 7). Hence, the polymer-tethered viologen should be able to accept electrons from the polymer-integrated hydrogenase. Moreover, this value is more negative than the reactivation potentials of the [NiFeSe] hydrogenase. From a

DOI: 10.1021/acsenergylett.7b00167
ACS Energy Lett. 2017, 2, 964−968

thermodynamic point of view, the viologen should be hence able to reduce the inactivated hydrogenase. It should be noted that, compared to the freely diffusing mediator **vio**, the potentials of both reductions (−451 and −683 mV, Figure S1, blue line) are shifted to more positive potentials in the case of the polymer-bound viologen unit (−295 and −660 mV, Figure S1, black line). Thus, the polymer matrix stabilizes the reduced forms of the mediator.

Figure 1a depicts cyclic voltammograms of a **P(N$_3$MA-BA-GMA)-vio**/*Dv*H-[NiFeSe] film drop cast onto a glassy carbon (GC) electrode under argon (black line) and H_2 atmospheres (red lines). Under an argon atmosphere, a chemically reversible redox couple of the first viologen reduction was observed (black curve). Under turnover conditions (red line, 100% H_2), a pronounced catalytic current response was detected, with a half-wave potential that closely matches the redox potential of the viologen moiety. Because the latter is ∼150 mV more positive than the $H_2/2H^+$ couple at pH 7.4, the enzyme is productively wired via the polymer-tethered viologen moieties and DET can be excluded. Moreover, steady-state currents were observed for high (100%, Figure 1a, red solid line) and low (5%, red dashed line) H_2 concentrations at potentials between ∼−0.2 and +0.2 V even for slow scan rates (2 mV s^{-1}, Figure S3a). We conclude that the redox polymer acts as a Nernst buffer and that high potential deactivation, which starts between −0.1 V and 0 V at low H_2 concentrations,[2,11] is absent. No significant loss of catalytic current was observed within a period of 16 h under continuous turnover conditions (Figure S3b), and the peak currents of the viologen moiety show almost identical intensity before and after the long-term experiment (Figure S3c). Moreover, electrodes that were prepared from the same enzyme batch show a similar catalytic response (Figure S4).

Figure 1b exhibits an $I-t$ curve of a drop-cast **P(N$_3$MA-BA-GMA)-vio**/*Dv*H-[NiFeSe] film measured at an applied potential of +160 mV (vs SHE) with 20% H_2/80% Ar bubbling through the electrolyte. At this H_2 partial pressure, the amount of H_2 in solution defines the catalytic current (Figure S5a), which is attributed to H_2 mass transport limitations within thick films.[16] Upon addition of 5% O_2 to the gas feed (5% O_2/20% H_2/75% Ar), the current decreases, indicating that electrons from the enzyme-catalyzed oxidation of H_2 are used by the viologen species to reduce incoming O_2.[14,16] Note that at this high potential O_2 is not reduced at the GC electrode (Figure S5b) but exclusively via the reduced viologen species. Alternating between the H_2/O_2/Ar and the H_2/Ar gas feeds reveals that the catalytic current for H_2 oxidation recovers during each anaerobic period (Figure 1b). In contrast, complete loss of the catalytic current is observed for enzymes wired in the DET regime.[2,11] These findings demonstrate protection of the [NiFeSe] hydrogenase and fully agree with our former results on the protection of [NiFe] and [FeFe] hydrogenases based on O_2 reduction properties of thick films.[14−16] However, the absolute currents decrease slightly with time. This behavior may be attributed to changes in the swelling state of the polymer/enzyme film. According to the models that were described in refs 16 and 20, the behavior of the films can be classified as regime III or case III. In regime III, the current under O_2/H_2 mixtures only depends on mass transport of the gases O_2 (D_O) and H_2 (D_S) as well as the film thickness l (eq 28a in ref 16)

$$J/F = (D_S S^\infty - D_O O^\infty)/l$$

where J = catalytic current, F = Faraday constant, D_S = diffusion coefficient of the substrate, $S = c$(substrate), D_O = diffusion coefficient of O_2, $O = c(O_2)$, and l = film thickness. Changes in this current may be associated with changes in the swelling state of the polymer (possibly due to local pH change accompanied by the catalytic reaction), which may affect l, D_O, $c(O_2)$, D_S, and/or $c(H_2)$. The difference in slope for anaerobic and aerobic current supports the assumption that O_2/H_2 mass transport contributes to changes and that a general decrease indicates a film thickness increase (swelling).

The question whether [NiFeSe] hydrogenase reactivation within the redox film can contribute to protection remains open. Reactivation of [NiFeSe] hydrogenases upon inhibition by O_2 is well-known for *Desulfomicrobium baculatum*[2] and for *Desulfovibrio vulgaris* Hildenborough[11] [NiFeSe] hydrogenases in the DET regime. Two inactive states are generated during oxidative (aerobic and anaerobic)[11] inactivation of [NiFeSe] hydrogenases; a so-called high potential reactivating species[2] or "fast" inactive state[11] as well as a low potential reactivating species[2] or "slow" inactive state,[11] which can be reactivated at potentials around ∼0 and ∼−0.35 V (vs SHE), respectively. Both are above or close to the redox potential of the polymer-bound viologen unit (∼−0.3 V).

Deactivation by O_2 and reactivation processes of an enzyme embedded in a redox matrix are best studied in thin polymer/enzyme layers to limit the contribution from protection through O_2 reduction (which increases with the film thickness[16]). However, the formation of very thin films by a common drop-cast process is difficult to achieve in a reproducible way. Hence, we applied a nonmanual deposition process based on electrochemical in situ activation of a protected bifunctional cross-linker, that is, trityl-protected 2,2′-(ethylenedioxy)-bis(ethylamine) (CL_p, Scheme 1b). Deprotection occurs by applying short positive potential pulses (+1.71 V vs SHE for 0.2 s), which lead to water splitting at the electrode surface and thus a change in the local pH value within the diffusion layer by generation of H^+ ions. Under these conditions, the pH-responsive trityl protecting groups are cleaved from the amino groups of the cross-linker (Scheme 1b). The activated cross-linker (Cl_a) starts then to react with the electrophilic epoxide functions within **P(N$_3$MA-BA-GMA)-vio** (Scheme 1b) and forms a dense, insoluble 3D network that is able to entrap the biocatalyst. The amount and hence the film thickness of the deposited polymer can be adjusted by varying the number n of repetitions of the applied potential pulse sequence. Between pulses, a potential of +0.21 V vs SHE was applied for 2 s to allow the reaction to proceed and to refresh the cross-linker and polymer concentration at the electrode surface. This led to a pulse sequence of n (+1.71 V/0.2 s; +0.21 V/2 s). Preliminary tests with the pure polymer revealed that the maximum loading of polymer with respect to the amount of viologen species on the electrode was obtained for n = 20−30 (Figure S6 and Table S1, the highest peak current and highest specific viologen surface concentration). Optical micrographs of the deposited films showed the deposition of many small polymer spots on the electrode surface rather than a homogeneous film (Figure S7). However, the amount of deposited material is substantially lower than that in the case of a drop-cast film. A closer inspection of the cyclic voltammograms revealed that only for n < 20 were very thin films that exhibit characteristics of an adsorption-controlled electron transfer reaction obtained (peak current ∝ scan rate, peak potential separation < 60 mV; see, e.g., Figure S6c,e).

DOI: 10.1021/acsenergylett.7b00167
ACS Energy Lett. 2017, 2, 964−968

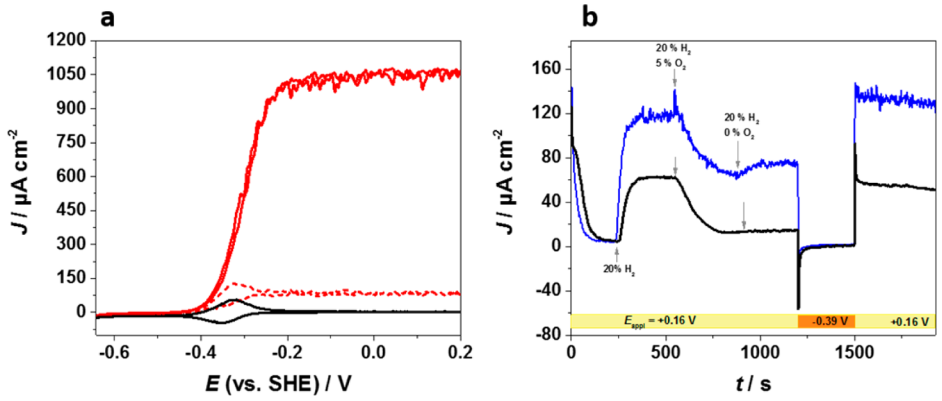

Figure 2. Cyclic voltammograms (a) and chronoamperogram (b) of thin P(N_3MA-BA-GMA)/*Dv*H-[NiFeSe] films prepared by electrochemical induced deposition applying the pulse sequence *n*(+1.71 V/0.2 s; +0.21 V/2 s), with *n* = number of repetitions; working electrolyte: PB (0.1 M, pH 7.4). (a) *n* = 20; scan rate: 10 mV s^{-1}; black line: 100% Ar; red solid line: 100% H_2; red dashed line: 5% H_2/95% Ar. (b) Applied potential: +0.16 or −0.39 V vs SHE (see graph); H_2/O_2 ratios were adjusted by varying the argon content in the gas flow; black trace: *n* = 2; blue trace: *n* = 10.

Consequently, to ensure the formation of thin polymer/enzyme layers, values of $n \leq 20$ were chosen for the co-deposition of *Dv*H-[NiFeSe] and **P(N_3MA-BA-GMA)-vio**. Figure 2a exhibits cyclic voltammograms of an electrochemically deposited **P(N_3MA-BA-GMA)-vio**/*Dv*H-[NiFeSe] film ($n = 20$) under 100% argon (black line) and 100% H_2 (red solid line). By calculating the charge from voltammograms recorded at a scan rate of 2 mV s^{-1} under nonturnover conditions, the surface concentration of viologen moieties Γ_{vio} was estimated to be 3.32 nmol cm^{-2}, which is ∼40 times lower than that for a drop-cast polymer film (Figure S2). A pronounced catalytic current response with a steady-state current above ∼−0.2 V was observed under turnover conditions, even for low H_2 concentrations (5% O_2, red dashed line) and for scan rates of 10 mV s^{-1}, demonstrating that the viologen-based redox matrix acts as a Nernst buffer even in thin films, which is in contrast to the DET regime, where high potential deactivation was observed at this scan rate.[2] The absolute catalytic currents correlate with *n* (Figure S8a), and even for small values ($n = 1$ or 2), pronounced catalytic currents were obtained (Figure S8b,c). Moreover, the fact that the catalytic current correlates with the number of applied deposition cycles *n* (Figure S8a) clearly demonstrates that the observed catalytic currents are limited by the amount of biocatalyst (for $n < 10$) on the electrode surface and mass transport is not the rate-limiting step.[20,21]

Chronoamperometry under 20% H_2/80% Ar (Figure 2b, black trace) of a very thin film deposited with $n = 2$ revealed that after adding O_2 to the gas feed ($t = 550$ s, 5% O_2/20% H_2/75% Ar) the enzyme within the film was fully deactivated within ∼300 s. In contrast to drop-cast films, no current was recovered when the O_2 feed was stopped ($t = 900$ s, 20% H_2/80% Ar), indicating that all enzyme molecules were deactivated. However, when a negative potential was applied to the electrode (−390 mV vs SHE, at $t = 1200$ to 1500 s) with 20% H_2/80% Ar bubbling through the cell, the oxidative current could be fully restored (at $t > 1500$ s). Obviously, the use of low-potential viologen moieties allows for reactivation of the enzymes, in analogy with observations in the DET regime. Because a DET between the electrode and the enzyme can be excluded for our system (no deactivation at high potentials), reactivation of the enzyme proceeds via the reduction of the inactive enzyme by the reduced viologen species. This was evidenced by experiments where potentials above the redox potential of the viologen moiety were applied after the O_2 flow was stopped (−0.1 and 0 V vs SHE, Figure S9a,b). In this case, reactivation was not observed for potentials of −0.1 V (Figure S9a) or 0 V (Figure S9b). Only when the potential was stepped to values more negative than the redox potential of the viologen (∼−0.3 V) could catalytic currents be restored (−0.39 V; Figure S9c).

It should be noted that no conclusion on the type and nature of the inactive state of the hydrogenases can be drawn because the potential of the viologen matrix (−0.295 V) is below or very close to the reactivation potentials of the low (∼−0.350 V) and high potential (∼0 V) reactivating species.[2,11]

The degree of current decay upon addition of O_2 clearly depends on the number of *n* used for polymer deposition and thus on the film thickness (Figures 2b and S10a−c). Films that were deposited with $n = 10$ (Figure 2b, blue trace) do not show complete deactivation upon addition of O_2 possibly due to increasing contribution from protection through O_2 reduction. This is backed by the fact that when the O_2 flux was stopped thick films showed at least partial recovery of the current (Figure S10e). Moreover, this demonstrates that deactivation is indeed based on inhibition by O_2 and not due to high potential deactivation that would occur in the DET regime. Reactivation is also possible under a pure argon atmosphere (Figure S10d,e). We conclude that for the viologen-induced reactivation process, the presence of H_2 is not a prerequisite.

In conclusion, the use of a low potential redox polymer ensures efficient protection of [NiFeSe] hydrogenase from *Desulfovibrio vulgaris* Hildenborough against O_2 and thus enables application of this particular enzyme as a catalyst for H_2 oxidation. Current densities of 1.0 and 1.7 mA cm^{-2}, obtained for thin (favorable mass transport) and thick (high catalyst loading) polymer/enzyme films, respectively, are the highest for hydrogenase incorporated in redox matrices. The low potential redox mediator does not only allow for protection through reduction of molecular oxygen but also enables reactivation of deactivated biocatalyst by transferring electrons to the inhibited enzyme, as was shown in thin films, deposited via an electrochemically induced cross-linking process. Our results clearly demonstrate that the combination of this particular hydrogenase and viologen-based redox hydrogels is

DOI: 10.1021/acsenergylett.7b00167
ACS Energy Lett. 2017, 2, 964−968

a very promising concept for use in energy conversion applications.

■ ASSOCIATED CONTENT

Supporting Information

The Supporting Information is available free of charge on the ACS Publications website at DOI: 10.1021/acsenergylett.7b00167.

Detailed protocols for syntheses of the redox polymer and all precursors, spectroscopic characterization, and additional electrochemical experiments (PDF)

■ AUTHOR INFORMATION

Corresponding Authors

*E-mail: adrian.ruff@ruhr-uni-bochum.de (A.R.).
*E-mail: wolfgang.schuhmann@ruhr-uni-bochum.de (W.S.).

ORCID

Adrian Ruff: 0000-0001-5659-8556
Nicolas Plumeré: 0000-0002-5303-7865
Wolfgang Schuhmann: 0000-0003-2916-5223

Notes

The authors declare no competing financial interest.

■ ACKNOWLEDGMENTS

This work was supported by the DFG within the framework of the Cluster of Excellence RESOLV (EXC 1069), by the DFG-ANR within the projects SHIELD PL746/2-1 and N° ANR-15-CE05-0020, by the European Commission within the Marie-Curie project "Bioenergy" (PITN-GA-2013-607793), and by the Fundação para a Ciência e Tecnologia (Portugal) (Grants UID/Multi/04551/2013, LISBOA-01-0145-FEDER-007660, PTDC/BBB-BEP/2885/2014 and Ph.D. fellowship SFRH/BD/100314/2014). N.P. acknowledges support by the European Research Council (ERC Starting Grant 715900). The authors thank Dr. Ines Ruff (Thermo Fisher Scientific) for IR measurements, Melinda Nolten (Ruhr-Universität Bochum) for help with the syntheses, and Prof. S. Ludwigs and Dr. K. Dirnberger (both University of Stuttgart, IPOC) for SEC measurements.

■ REFERENCES

(1) Wombwell, C.; Caputo, C. A.; Reisner, E. NiFeSe-hydrogenase chemistry. *Acc. Chem. Res.* **2015**, *48*, 2858−2865.

(2) Parkin, A.; Goldet, G.; Cavazza, C.; Fontecilla-Camps, J. C.; Armstrong, F. A. The difference a Se makes? Oxygen-tolerant hydrogen production by the NiFeSe-hydrogenase from *Desulfomicrobium baculatum*. *J. Am. Chem. Soc.* **2008**, *130*, 13410−13416.

(3) Reisner, E.; Fontecilla-Camps, J. C.; Armstrong, F. A. Catalytic electrochemistry of a NiFeSe-hydrogenase on TiO_2 and demonstration of its suitability for visible-light driven H_2 production. *Chem. Commun.* **2009**, 550−552.

(4) Reisner, E.; Powell, D. J.; Cavazza, C.; Fontecilla-Camps, J. C.; Armstrong, F. A. Visible light-driven H_2 production by hydrogenases attached to dye-sensitized TiO_2 nanoparticles. *J. Am. Chem. Soc.* **2009**, *131*, 18457−18466.

(5) Sakai, T.; Mersch, D.; Reisner, E. Photocatalytic hydrogen evolution with a hydrogenase in a mediator-free system under high levels of oxygen. *Angew. Chem., Int. Ed.* **2013**, *52*, 12313−12316.

(6) Caputo, C. A.; Gross, M. A.; Lau, V. W.; Cavazza, C.; Lotsch, B. V.; Reisner, E. Photocatalytic hydrogen production using polymeric carbon nitride with a hydrogenase and a bioinspired synthetic Ni catalyst. *Angew. Chem., Int. Ed.* **2014**, *53*, 11538−11542.

(7) Baltazar, C. S. A.; Marques, M. C.; Soares, C. M.; DeLacey, A. M.; Pereira, I. A. C.; Matias, P. M. Nickel-Iron-Selenium hydrogenases - An overview. *Eur. J. Inorg. Chem.* **2011**, *2011*, 948−962.

(8) Gutierrez-Sanchez, C.; Rüdiger, O.; Fernandez, V. M.; De Lacey, A. L.; Marques, M.; Pereira, I. A. C. Interaction of the active site of the Ni-Fe-Se hydrogenase from *Desulfovibrio vulgaris* Hildenborough with carbon monoxide and oxygen inhibitors. *JBIC, J. Biol. Inorg. Chem.* **2010**, *15*, 1285−1292.

(9) Marques, M. C.; Coelho, R.; Pereira, I. A.; Matias, P. M. Redox state-dependent changes in the crystal structure of [NiFeSe] hydrogenase from *Desulfovibrio vulgaris* Hildenborough. *Int. J. Hydrogen Energy* **2013**, *38*, 8664−8682.

(10) Fontecilla-Camps, J. C.; Volbeda, A.; Cavazza, C.; Nicolet, Y. Structure/function relationships of NiFe- and FeFe-hydrogenases. *Chem. Rev.* **2007**, *107*, 4273−4303.

(11) Ceccaldi, P.; Marques, M. C.; Fourmond, V.; Pereira, I. C.; Leger, C. Oxidative inactivation of NiFeSe hydrogenase. *Chem. Commun.* **2015**, *51*, 14223−14226.

(12) Rüdiger, O.; Gutiérrez-Sánchez, C.; Olea, D.; Pereira, I. A. C.; Vélez, M.; Fernández, V. M.; De Lacey, A. L. Enzymatic anodes for hydrogen fuel cells based on covalent attachment of Ni-Fe hydrogenases and direct electron transfer to SAM-modified gold electrodes. *Electroanalysis* **2010**, *22*, 776−783.

(13) Tapia, C.; Zacarias, S.; Pereira, I. A. C.; Conesa, J. C.; Pita, M.; De Lacey, A. L. In Situ Determination of photobioproduction of H_2 by In_2S_3-[NiFeSe] hydrogenase from *Desulfovibrio vulgaris* Hildenborough using only visible light. *ACS Catal.* **2016**, *6*, 5691−5698.

(14) Plumeré, N.; Rüdiger, O.; Oughli, A. A.; Williams, R.; Vivekananthan, J.; Pöller, S.; Schuhmann, W.; Lubitz, W. A redox hydrogel protects hydrogenase from high-potential deactivation and oxygen damage. *Nat. Chem.* **2014**, *6*, 822−827.

(15) Oughli, A. A.; Conzuelo, F.; Winkler, M.; Happe, T.; Lubitz, W.; Schuhmann, W.; Rüdiger, O.; Plumeré, N. A redox hydrogel protects the O_2-sensitive FeFe-hydrogenase from *Chlamydomonas reinhardtii* from oxidative damage. *Angew. Chem., Int. Ed.* **2015**, *54*, 12329−12333.

(16) Fourmond, V.; Stapf, S.; Li, H.; Buesen, D.; Birrell, J.; Rüdiger, O.; Lubitz, W.; Schuhmann, W.; Plumeré, N.; Leger, C. Mechanism of protection of catalysts supported in redox hydrogel films. *J. Am. Chem. Soc.* **2015**, *137*, 5494−5505.

(17) Morozov, S.; Voronin, O.; Karyakina, E.; Zorin, N.; Cosnier, S.; Karyakin, A. Tolerance to oxygen of hydrogen enzyme electrodes. *Electrochem. Commun.* **2006**, *8*, 851−854.

(18) Marques, M. C.; Tapia, C.; Gutiérrez-Sanz, O.; Ramos, A. R.; Keller, K. L.; Wall, J. D.; De Lacey, A. L.; Matias, P. M.; Pereira, I. A. C. The direct role of selenocysteine in [NiFeSe] hydrogenase maturation and catalysis. *Nat. Chem. Biol.* **2017**, DOI: 10.1038/nchembio.2335.

(19) Pöller, S.; Koster, D.; Schuhmann, W. Stabilizing redox polymer films by electrochemically induced crosslinking. *Electrochem. Commun.* **2013**, *34*, 327−330.

(20) Bartlett, P. N.; Pratt, K. Theoretical treatment of diffusion and kinetics in amperometric immobilized enzyme electrodes Part I: Redox mediator entrapped within the film. *J. Electroanal. Chem.* **1995**, *397*, 61−78.

(21) Andrieux, C. P.; Dumas-Bouchiat, J. M.; Savéant, J. M. Catalysis of electrochemical reactions at redox polymer electrodes. *J. Electroanal. Chem. Interfacial Electrochem.* **1982**, *131*, 1−35.

DOI: 10.1021/acsenergylett.7b00167
ACS Energy Lett. 2017, 2, 964−968